

Fractals **3**, 483-390 (1995) [also published in: "Fractal geometry and analysis - The Mandelbrot Festschrift, Curacao 1995", C. J. G. Evertsz, H.-G. Peitgen, and R. F. Voss (Eds.) (World Scientific, Singapore, 1996) p. 79-86]

Fractal Aspects in Polymer Science

H. Schiessel and A. Blumen

Theoretical Polymer Physics, Freiburg University, Rheinstr. 12, D-79104 Freiburg, Germany

ABSTRACT: Scaling aspects are of common occurrence in polymer science. Here we concentrate on the fractal behavior of dynamical systems. As examples we focus on the sol-gel transition and on the patterns of motion displayed by polyampholytes (polymers containing positive and negative charges).

1. Introduction

Scaling laws are ubiquitous in polymer science, so that it comes as no surprise that fractal concepts find here very fruitful grounds. Many structural aspects are fractal: Thus in good solvents, under excluded volume conditions, the average squared end-to-end distance of a chain is a power-law of the number of monomers [1], fact which translates into a fractal relation [2]. Less emphasized is the fact that also dynamical processes in polymers show fractal behavior. A basic example is photoconductivity, in which charge carriers undergo dispersive transport, often such that the diffusion coefficient displays an algebraic dependence on time [3]. As pointed out by Mandelbrot (cf. p. 417ff of Ref. [2]) scaling decays, i.e. hyperbolic relaxation patterns

$$\Phi(t) \propto t^{-\gamma} \quad (1)$$

with $0 < \gamma < 1$ are commonly found in physical systems as a response to external perturbations. As further typical processes which obey Eq. (1) we mention the stress relaxation in viscoelastic materials [4], especially in critical gels [5], the dielectric relaxation in liquids [6] and the current behavior at rough electrode-electrolyte interfaces [7].

Mimicking the decay law, Eq. (1), through a superposition of exponentials, e.g.

$$\Phi(t) = \int_0^{\infty} \rho(\tau) \exp(-t/\tau) d\tau, \quad (2)$$

(where $\rho(\tau)$ gives the distribution of relaxation times) is conceptually not satisfactory [2]. On the other hand, one expects that the exponent γ mirrors in some way the properties of the underlying medium. There are a series of approaches which relate the exponent γ to dynamical aspects, such as the continuous-time random walk (CTRW), where γ appears in the waiting-time distribution [8] or, in a more subtle connection, expressions involving fractional calculus [9]. In a series of works [10-12] we have shown how fractional derivatives may be related in a straightforward way to an underlying hierarchical structure. In Ref. [12] we have used such hierarchical models (ladder-like and fractal spring-dashpot arrangements) in order to describe the dynamics observed during gelation.

1. Ladder and Fractal Arrangements

In this section we introduce mechanical networks which mimic the viscoelastic and the structural properties at the sol-gel transition. Crosslinking polymers at the gel point show in general a power law behavior of the complex modulus

$$G^*(\omega) \propto (i\omega)^\gamma \quad (3)$$

with $0 < \gamma < 1$ over many decades in frequency. Relation (3) implies for the relaxation modulus $G(t)$, given by $G^*(\omega) = i\omega \int_0^\infty G(\tau) \exp(-i\omega\tau) d\tau$, an algebraic decay, Eq. (1).

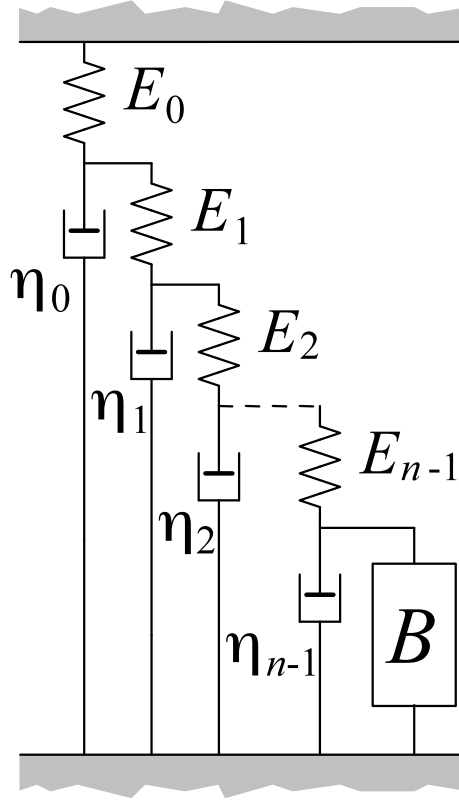


Fig. 1 Ladder arrangement used to model scaling decays.

In Fig. 1 we display mechanical arrangements which lead to algebraic relaxation forms. The models consist of ladder-like structures with springs (having spring constants E_0, E_1, E_2, \dots) along one of the struts and dashpots (with viscosities $\eta_0, \eta_1, \eta_2, \dots$) on the rungs of the ladder. Here we examine three different forms of ladder models: (a) a finite ladder structure, obtained by replacing in Fig. 1 the box B by a spring E_n and a dashpot η_n in series (a so-called Maxwell element (E_n, η_n)), (b) an infinite arrangement, in which case the box B in Fig. 1 represents a non-terminating ladder and (c) a finite ladder structure, obtained by using a spring as the final rung (here the box B consists simply in a spring E_n).

As in Ref. [10] we obtain for the complex modulus $G^*(\omega)$ continued fraction expressions. The complex modulus of the infinite ladder, case (b), fulfils

$$G^*(\omega) = \frac{E_0}{1+} \frac{(i\omega)^{-1} \frac{E_0}{\eta_0}}{1+} \frac{(i\omega)^{-1} \frac{E_1}{\eta_0}}{1+} \frac{(i\omega)^{-1} \frac{E_1}{\eta_1}}{1+} \dots, \quad (4)$$

whereas the finite arrangement (a) leads to the terminating continued fraction

$$G^*(\omega) = \frac{E_0}{1+} \frac{(i\omega)^{-1} \frac{E_0}{\eta_0}}{1+} \frac{(i\omega)^{-1} \frac{E_1}{\eta_0}}{1+} \dots \frac{(i\omega)^{-1} \frac{E_n}{\eta_{n-1}}}{1+} \frac{(i\omega)^{-1} \frac{E_n}{\eta_n}}{1} \quad (5)$$

and case (c) to the expression:

$$G^*(\omega) = \frac{E_0}{1+} \frac{(i\omega)^{-1} \frac{E_0}{\eta_0}}{1+} \frac{(i\omega)^{-1} \frac{E_1}{\eta_0}}{1+} \dots \frac{(i\omega)^{-1} \frac{E_{n-1}}{\eta_{n-1}}}{1+} \frac{(i\omega)^{-1} \frac{E_n}{\eta_{n-1}}}{1}. \quad (6)$$

Choosing in Eq. (4) $E_0 = E_1 = \dots = E$ and $\eta_0 = \eta_1 = \dots = \eta$ it can be shown (by comparing terminating approximations of the continued fraction with the binomial series) that the complex modulus of the infinite arrangement is given by

$$G^*(\omega) = E \frac{(4(i\omega\tau)^{-1} + 1)^{1/2} - 1}{2(i\omega\tau)^{-1}} \quad (7)$$

where we set $\tau = \eta/E$. For $\omega\tau \ll 1$ Eq. (7) reduces to the form $G^*(\omega) \cong E(i\omega\tau)^{1/2}$. Therefore having the same spring constants and viscosities for the whole arrangement one gets a complex modulus with $\gamma = 1/2$. The short time behavior (i.e. $\omega\tau \gg 1$) is dominated by the first spring of the ladder and models a solid-like, glassy behavior with $G'(\omega) \cong E$ and $G''(\omega) \cong E(\omega\tau)^{-1}$. Of interest are furthermore the long-time dynamics ($\omega\tau \ll 1/n^2$) for the finite arrangements (cases (a) and (c)). In case (a) one obtains from Eq. (5) a fluid-like behavior whose steady-flow viscosity is $\eta_f = (n+1)\eta$. In case (c), Eq. (6), one finds that the equilibrium modulus $G_\infty = (n+1)^{-1}E$ does not vanish, i.e. the system behaves like a solid. Case (a) is hence typical for a pregel and case (c) for a postgel [12].

To obtain other values for γ , a suitable distribution for the spring constants and viscosities has to be chosen (for instance an algebraic k -dependence with

$E_k \propto \eta_k \propto k^{1-2\gamma}$ [10]). Such an arbitrary choice of the material constants is, however, reminiscent of the "distributed times panacea" [2].

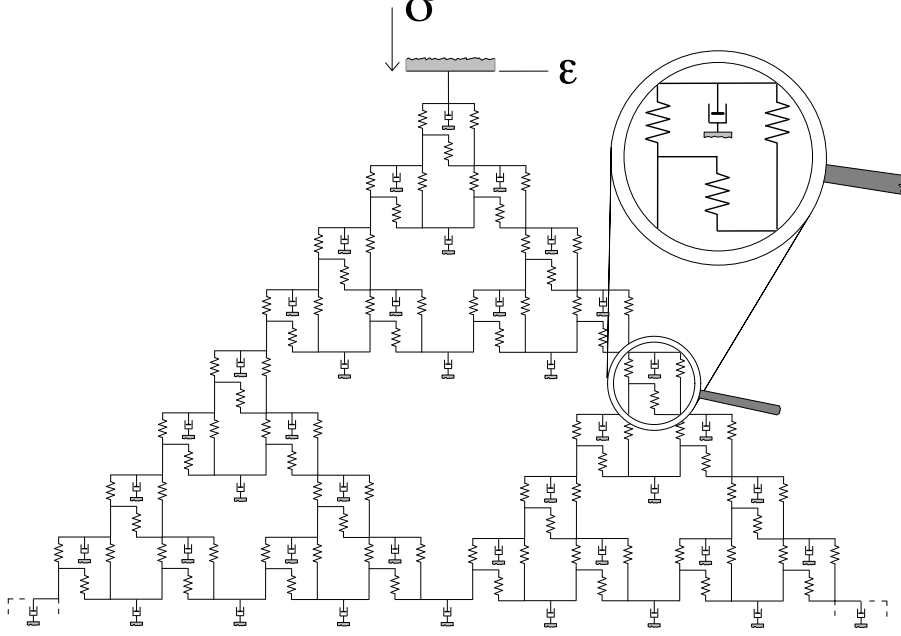


Fig. 2 Section of the infinite mechanical network based on the Sierpinski gasket.

We prefer to proceed by showing that other γ -values arise from fractal arrangements. The construction starts by connecting each site \mathbf{r}_i of a given fractal network to neighboring nodes \mathbf{r}_j by equal springs with spring constant E and linking each \mathbf{r}_i to the ground via a site-dependent dashpot with viscosity $\eta_i = z(\mathbf{r}_i)\eta$ (where $z(\mathbf{r}_i)$ is the coordination number of node \mathbf{r}_i). Furthermore, the nodes' motion is perpendicular to the ground. To give an example we show in Fig. 2 a section of the infinite mechanical network constructed from the Sierpinski gasket [2]. The analogy to random walks can now be seen by comparing the stresses acting on node \mathbf{r}_i (whose displacement is ε_i)

$$\eta_i \dot{\varepsilon}_i(t) = E \sum_{j(i)} [\varepsilon_j(t) - \varepsilon_i(t)] \quad (8)$$

with the master equation

$$\frac{dP(\mathbf{r}_i, t)}{dt} = \sum_{j(i)} [w_{ij}P(\mathbf{r}_j, t) - w_{ji}P(\mathbf{r}_i, t)] \quad (9)$$

which governs the probability $P(\mathbf{r}_i, t)$ of having a random walker at site \mathbf{r}_i . In Eqs. (8) and (9) the sums run over all nearest neighbours \mathbf{r}_j of \mathbf{r}_i . The transition probabilities w_{ij} in Eq. (9) obey $z(\mathbf{r}_j)w_{ij} = w = \text{constant}$. One can now identify formally $\eta_i \varepsilon_i(t)$ with $P(\mathbf{r}_i, t)$. Furthermore, the probability for a random walker to return to the origin at time t follows an algebraic form:

$$P(t) \propto t^{-d_s/2} \quad (10)$$

where d_s is the spectral dimension of the network. It follows [12] a power law behavior of the complex modulus, Eq. (3), with $\gamma = 1 - d_s/2$. The ladder model, Fig. 1, is the special case of a one-dimensional lattice with $d_s = 1$ and thus $\gamma = 1/2$; the Sierpinski gasket in 2d has $d_s = 2\ln(3)/\ln(5)$ and hence $\gamma = 1 - \ln(3)/\ln(5) \cong 0.317$.

Now, ladder and fractal arrangements allow to display how the mechanical properties of crosslinked systems depend on their stage of gelation [12]. First, the relation $\gamma = 1 - d_s/2$ connects the dynamics with the topological properties of the fractal. Second, the fluid- or solid-like behaviors encountered in pre- or postgels, respectively are related to the cut-off parameters of the self-similar structure. The experimental findings indicate that γ changes during the sol-gel transition [5] fact directly related to the geometrical changes in the underlying chemical network during gelation.

3. Dynamics of Polyampholytes (PA)

In this section we present our results on the behavior of PAs in external electrical fields [13]. We follow the lines of Ref. [13] and view the PA as consisting of N charged beads, connected into a linear chain by harmonic springs. The chain's position is given by the set $\{\mathbf{R}_n(t)\}$, where $\mathbf{R}_n(t) = (X_n(t), Y_n(t), Z_n(t))$ is the position

vector of the n th bead ($n = 0, 1, \dots, N-1$) at time t . We denote the charge of the n th bead by q_n and take it to be a quenched random variable. The potential energy is then:

$$U(\{\mathbf{R}_n(t)\}) = \frac{K}{2} \sum_{n=1}^{N-1} [\mathbf{R}_n(t) - \mathbf{R}_{n-1}(t)]^2 - \mathbf{E} \sum_{n=0}^{N-1} q_n \mathbf{R}_n(t). \quad (11)$$

In Eq. (11) \mathbf{E} denotes the electrical field and $K = 3T/b^2$ the spring constant; T is the temperature in units of the Boltzmann constant k_B and b is the mean distance between beads (in the absence of an external field). The electrical field points along the Y -axis, so that $\mathbf{E} = (0, E, 0)$ holds. Eq. (11) turns into the Rouse model when excluded volume effects and hydrodynamic interactions are disregarded; then the chain's dynamics is described by N coupled Langevin equations [14-16]

$$\zeta \frac{d\mathbf{R}_n(t)}{dt} = - \frac{\partial U(\{\mathbf{R}_n(t)\})}{\partial \mathbf{R}_n(t)} + \mathbf{f}_R(n, t). \quad (12)$$

In Eq. (12) ζ is the friction constant and $\mathbf{f}_R(n, t)$ are Gaussian random forces with $\overline{f_i(n, t)} = 0$ and $\overline{f_i(n, t) f_j(n', t')} = 2\zeta T \delta_{ij} \delta_{nn'} \delta(t - t')$. Here i and j denote the components of the force vector, i.e. $i, j = X, Y, Z$ and the dash stands for the thermal averages, i.e. averages over realizations of the Langevin forces $\mathbf{f}_R(n, t)$.

One obtains now readily [13] the explicit time dependence of the mean squared displacement (MSD) of the chain's center of mass (CM), the average squared end-to-end distance and the MSD of a tagged bead. Thus the following result for the MSD of the CM in the Y -direction holds:

$$\overline{\langle (Y_{CM}(t) - Y_{CM}(0))^2 \rangle} = \frac{2T}{\zeta N} t + \frac{E^2}{\zeta^2} \langle \tilde{q}_0^2 \rangle t^2. \quad (13)$$

In Eq. (13) the brackets denote averages with respect to the realizations of q_n and use was made of the properties of $f_i(n, t)$; furthermore $\langle \tilde{q}_0^2 \rangle$ is the pair correlation function of the charge variable, and $\tilde{q}_p = N^{-1} \int_0^N dn \cos(p\pi n/N) q_n$ the Fourier transform of the q_n .

Furthermore, the Y -component of the end-to-end vector $\mathbf{P}(t) = \mathbf{R}_0(t) - \mathbf{R}_N(t)$ obeys:

$$\overline{\langle P_Y^2(t) \rangle} = \frac{b^2 N}{3} + \frac{16 E^2}{\zeta^2} \sum_{\hat{p}} \sum_{\hat{q}} \langle \tilde{q}_{\hat{p}} \tilde{q}_{\hat{q}} \rangle \int_0^t d\tau_1 \int_0^t d\tau_2 \exp(-p^2 \tau_1 / \tau_R - q^2 \tau_2 / \tau_R). \quad (14)$$

Here $\tau_R = \zeta b^2 N^2 / 3 \pi^2 T$ is the Rouse-time and the hat designates that the sum extends over odd, positive numbers only.

Depending on the distributions of the charge variables q_n a multitude of scaling laws follows [13]. As an example, consider the dynamics of a tagged bead, say one of the chain's end; its motion obeys a closed-form expression, which in full generality is rather complex [13]. Exemplarily, we show here the expression for the special case in which only the first bead of the PA is charged:

$$\overline{Y_0(t)} = \frac{qE}{\zeta N} t + \frac{2qE}{\zeta N} \sum_{p=1}^{\infty} \int_0^t d\tau \exp(-p^2 \tau / \tau_R). \quad (15)$$

For $t \ll \tau_R$ it follows

$$\overline{Y_0(t)} = \frac{qE}{\zeta N} t + \frac{2}{\sqrt{\pi}} \frac{qE}{\sqrt{\zeta K}} t^{1/2}, \quad (16)$$

For long chains $\tau_R \propto N^2 \gg 1$, so that $\overline{Y_0(t)} \propto t^{1/2}$ holds for a very long time. Evidently this is the PA's response to a field $E(t) = E \Theta(t)$, where Θ is the Heaviside step function. Then the position of the charged bead in the presence of an arbitrary external field $E(t)$ (with $E(t) = 0$ for $t \leq 0$) is well approximated by the following convolution integral

$$\overline{Y_0(t)} = \frac{q}{\sqrt{\zeta K}} \frac{1}{\Gamma(\alpha)} \int_0^t d\tau (t - \tau)^{\alpha-1} \frac{dE(\tau)}{d\tau} = \frac{q}{\sqrt{\zeta K}} \frac{d^{-\alpha}}{dt^{-\alpha}} \left[\frac{dE(t)}{dt} \right] \quad (17)$$

with $\alpha = 3/2$. The convolution integral of Eq. (17) is a *Riemann-Liouville integral* which for any $\alpha > 0$ defines the *fractional integral*, symbolized by the operator $d^{-\alpha}/dt^{-\alpha}$ [9]. Now *fractional derivatives* d^{α}/dt^{α} (for $\alpha > 0$) are obtained by applying ordinary derivatives to fractional integrals. Using the composition rule (see Ref. [9] for details) the following fractional differential equation follows:

$$qE(t) = \sqrt{\zeta K} \frac{d^{1/2} \overline{Y_0(t)}}{dt^{1/2}}. \quad (18)$$

This is a fractional relation which is very akin to the stress-strain expression

$$\sigma(t) = \eta^\gamma E^{1-\gamma} \frac{d'\varepsilon(t)}{dt'} \quad (19)$$

for which, in the ladder model, $\gamma = 1/2$ [10, 12]. The use of expressions such as Eq. (19) is of growing interest in the theory of viscoelasticity [4, 17, 18]. Now, is the similarity between Eqs. (18) and (19) accidental? No, the physical situation of the Rouse chain is, in fact similar to that of the ladder arrangement, Fig. 1. By performing the average over the Langevin forces in Eq. (15), we have $\overline{X_n(t)} = \overline{Z_n(t)} = 0$; this corresponds to a projection of the beads' average positions on the Y -axis (cf. Fig. 3). Furthermore these objects (due to the assumptions of the Rouse model) are connected by springs and are exposed to a velocity dependent friction, just as the elements of the ladder model. Mathematically the ladder model and the Rouse chain (and therefore Eq. (18) and Eq. (19) with $\gamma = 1/2$) are equivalent if one identifies the stress σ with the electrical force qE and the deformation ε with the thermal average of the charge's position, $\overline{Y_0}$.

4. Conclusion

In this work we have investigated relaxation processes on underlying self-similar structures. As a prototype we examined sequential ladder arrangements which lead to scaling decays with $\gamma = 1/2$. Furthermore, we have discussed fractal networks, where the relaxation exponent γ mirrors the connectivity of the lattice. As shown, these models can be applied to a broad range of physical systems, such as to critical gels and to polymers in electrical fields.

Acknowledgements: We are especially indebted to Dr. G. Oshanin for fruitful discussions and for his cooperation in establishing many of the results in Sec. 3. We acknowledge support by the Deutsche Forschungsgemeinschaft (SFB 60) and by the Fonds der Chemischen Industrie.

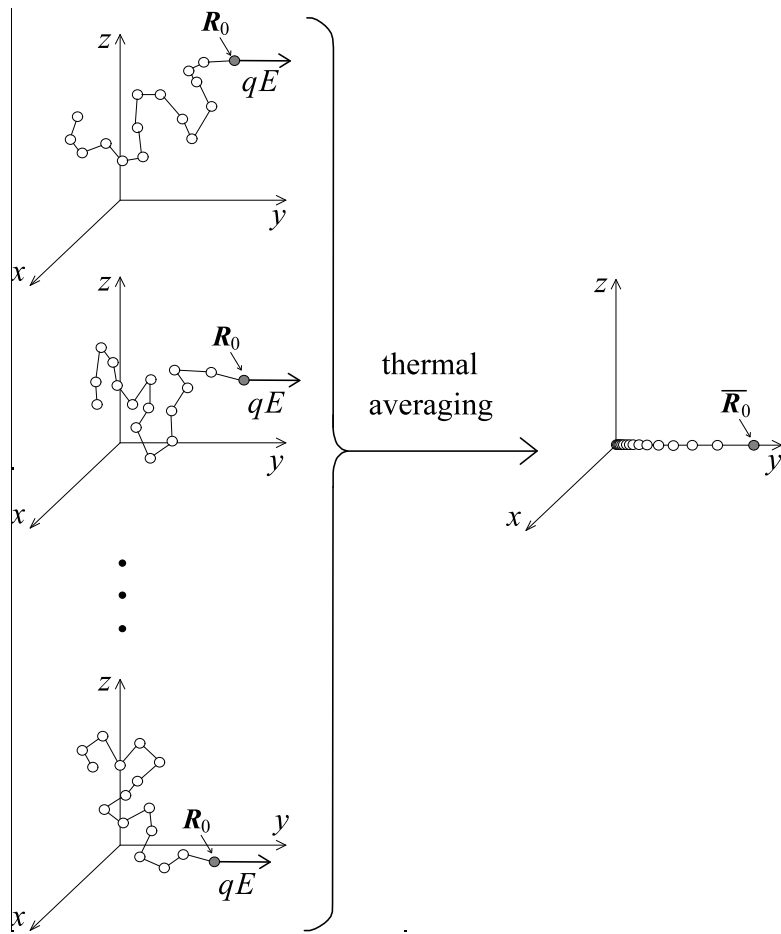


Fig. 3 Behavior of a Rouse chain under different realizations of the Langevin forces. The chain has one charged bead at \mathbf{R}_0 and is placed in a constant electrical field $\mathbf{E} = (0, E, 0)$. The averaging (depicted on the right-side) is equivalent to a projection on the Y -axis, see text for details.

References

- [1] P. J. Flory, *J. Chem. Phys.* **17**, 303 (1949).
- [2] B. B. Mandelbrot, *The Fractal Geometry of Nature* (Freeman, San Francisco, 1982).
- [3] A. Blumen and H. Schnörer, *Angew. Chem. Intern. Ed.* **29**, 113 (1990).
- [4] C. Friedrich and H. Braun, *Rheol. Acta* **31**, 309 (1992).
- [5] J. C. Scanlan and H. H. Winter, *Macromolecules* **24**, 47 (1991).
- [6] K. S. Cole and R. H. Cole, *J. Chem. Phys.* **9**, 341 (1941).
- [7] R. D. Armstrong and R. A. Burnham, *J. Electroanal. Chem.* **72**, 257 (1976).
- [8] H. Scher and E. W. Montroll, *Phys. Rev. B* **12**, 2455 (1975).
- [9] K. B. Oldham and J. Spanier, *The Fractional Calculus* (Academic Press, New York London, 1974).
- [10] H. Schiessel and A. Blumen, *J. Phys. A* **26**, 5057 (1993).
- [11] H. Schiessel, P. Alemany and A. Blumen, *Progr. Colloid Polym. Sci.* **96**, 16 (1994).
- [12] H. Schiessel and A. Blumen, *Macromolecules*, in press.
- [13] H. Schiessel, G. Oshanin and A. Blumen, submitted to *J. Chem. Phys.*
- [14] P. E. Rouse, *J. Chem. Phys.* **21**, 1272 (1953).
- [15] M. Doi and S. F. Edwards, *The Theory of Polymer Dynamics* (Clarendon Press, Oxford, 1986).
- [16] G. Oshanin and A. Blumen, *Phys. Rev. E* **49**, 4185 (1994).
- [17] W. G. Glöckle and T. F. Nonnenmacher, *Rheol. Acta* **33**, 337 (1994).
- [18] N. Heymans and J.-C. Bauwens, *Rheol. Acta* **33**, 210 (1994).